Winds and Wave Motions to 110 km at Mid-Latitudes
I. Partial Reflection Radiowave Soundings, 1972–73

A. H. MANSON, J. B. GREGORY AND D. G. STEPHENSON

Institute of Space and Atmospheric Studies, University of Saskatchewan, Saskatoon, Canada S7N 0W0

(Manuscript received 6 November 1973, in revised form 10 June 1974)

ABSTRACT

Measurements of winds (60–110 km) for Saskatoon, Canada (52N, 107W), have been obtained from a partial reflection radiowave system. Closely spaced atmospheric soundings (12 per hour) for heights between 51–117 km with 3-km height resolution, were made between August 1972 and September 1973. The median of the wind profiles for a given hour has been identified mainly as the prevailing wind, and the irregular components from each profile as internal atmospheric gravity waves ($30<\tau<60$ min, $12<\lambda_z<30$ km). The amplitudes and shears of the irregular winds have their largest values in winter. A diurnal variation has been found, showing a minimum in amplitude and shear values near noon for all seasons; this variation is especially noticeable above 90 km.

Comparisons of seasonal variations in the prevailing zonal and meridional winds, with the amplitudes of the irregular winds, suggest interactions involving critical layers and momentum transfer. Tropospheric weather systems are considered in relation to the gravity wave amplitudes.

1. Introduction

This paper presents results from a program of radiowave drift (wind) measurements from 60 km up to and including the ionospheric E region, for a location at 52N, 107W (Park Observatory, near Saskatoon). In an earlier paper (Gregory and Rees, 1971) a time cross section of zonal winds above 60 km, for February–June, 1969, was presented. ROCOB data from 54N, 110W, up to 60 km, were used to complete the profiles. Satisfactory agreement between these sets of data and recent models of zonal and meridional winds was demonstrated. Since that time, four years data have been assembled and analyzed, the winter months for each year having received the most intensive study. The weekly and monthly median wind profiles for these years will be discussed in a later paper in this series.

During 1972, an improved digital sampling system was developed (Gregory and Stephenson, 1972). This has allowed more rapid sounding of the atmosphere (12 per hour), and the resolution of small-period atmospheric waves in the internal atmospheric gravity wave spectrum (Manson *et al.*, 1973). In this first paper of the series, the rapid soundings for 1972-73 are discussed. The conclusions of this study will be of use in the interpretation of data from previous years.

2. Radiowave analysis and observations

a. Individual wind profiles

The wind data have been obtained at a radio frequency of 2.2 MHz, by application of the spaced antenna technique to partial reflections (Fraser, 1968; Gregory and Rees, 1971). Values of the wind, for various gated heights, were determined from the time delays for maximum correlation of data sequences for pairs of antennas. This method has been termed "numerical correlation." Three time shifts between pairs of antennas may be evaluated, permitting three estimates of velocity, of which only one is independent. In the present work, the median of the three vectors has been used, and the dispersion of the directions of the estimated vectors has been used in editing the data.

The detailed method of analysis of the radiowave data has been discussed by Manson *et al.* (1973) and Gregory *et al.* (1973). In brief, two stages of selection for the data are employed. In the first, selection criteria were incorporated in the computer processing of the sequences. These involved rejection of data for receiver saturation and low signal-to-noise conditions. The second stage of selection was carried out by inspection, when radio interference and other receiver saturation effects were eliminated. Following these various editing procedures, the wind vectors are of physically acceptable magnitude when compared with rocket data, and have low angular dispersion (typically less than 25°). The maximum value of dispersion acceptable for the retention of any wind estimate was 145°, but this criteria led to the rejection of little data.

b. Observations

Soundings were carried out between September 1972 and August 1973. In the improved sampling system,

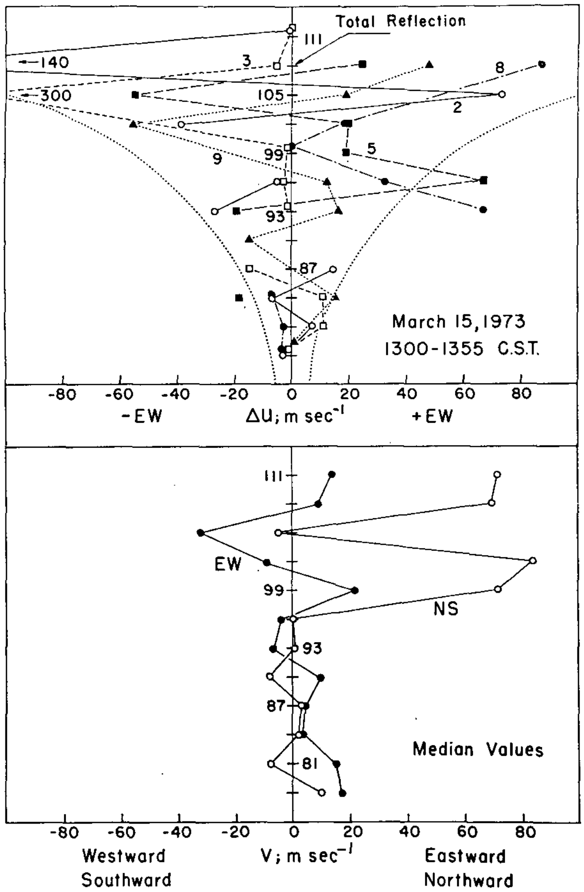

FIG. 1. Irregular wind profiles (upper) and median wind profiles (lower) for an intensive run from 1300–1355 CST 15 March 1973. The time sequence is from 1 to 12.

gates of 40 m width are spaced at 3-km intervals, from 51 to 117 km. Since the radiowave pulse width is 20 μsec, errors introduced by the double sampling of pulses are eliminated, and height resolution is $\sim$3 km (Manson *et al.*, 1973). Various sounding rates are available from this system (Gregory and Stephenson, 1972), with the limitation that 3 min of data are required at a given height for a determination of the wind. During the observing period, 12 complete altitude soundings per hour was the usual operating rate. The pattern of observations involved a 1-hr intensive sequence near noon two days per week, usually Wednesdays and Thursdays. In addition, diurnal sequences were attempted several days per month. These involved six intensive sequences spaced by 4 hr.

3. Winds analysis

a. Mean and irregular wind components

A median profile was obtained, for the wind profiles from any one intensive sequence of soundings, and the vector differences between individual profiles and the median were calculated. It is proposed that the median profiles be identified mainly with the prevailing winds for the appropriate observing periods, and the 12 differenced profiles be identified with the irregular winds for that hour. The association of the 1-hr median profile with the prevailing winds (plus a smaller tidal component) appeared justified following comparisons with winds from other zonal and meridional time cross sections (Gregory and Rees, 1971; Groves, 1969). Also, several consecutive intensive sequences have demonstrated small changes between the resulting median profiles (<10 m sec^{-1}), and hence it appears that little contribution due to longer period gravity waves ($\tau \approx 2$ hr) is present. In contrast, daily and weekly changes are found to be considerable and systematic.

b. Tidal components

An attempt was also made to analyze the diurnal sequences, involving as many as six median wind profiles, to obtain tidal components. Some fair comparisons with the expected semi-diurnal and diurnal tide combinations for this latitude (Chapman and Lindzen, 1970) were obtained, but the results have not yet shown a desirable statistical significance for presentation. Technical problems and auroral activity prevented diurnal sequences of sufficient continuity.

However, the results obtained indicated that the diurnal wind components at 53N, 107W have amplitudes of 10–15 m sec^{-1}, and that semi-diurnal and diurnal tidal components are of comparable magnitude. They demonstrate clockwise and counterclockwise rotation with height, and also considerable variability of phase over a period of several weeks (cf. Stubbs, 1973; Elford, 1959). Finally, both theory and observation suggest that the tidal contributions to the median (hourly) profiles are small at local noon, especially for the zonal flow, so that the identification of the median profiles with the prevailing winds is considered justified.

4. Irregular wind/gravity wave data

Examples of the median and irregular wind profiles obtained on two occasions are shown in Figs. 1 and 2. The lower portions of the figures present the median zonal and meridional profiles for the hour, and the upper portion the irregular wind components. The apparent height of total reflection in the E region at 2.2 MHz is shown, as well as the velocity profile appropriate to a propagating wave of constant energy density. The east-west and north-south irregular components are shown in Figs. 1 and 2, respectively, since they are considered to best show horizontal and vertical phase progression. [They are comparable in quality with observations discussed in Manson *et al.* (1973).] The other components are of comparable magnitude, revealing no significant indication of directional filtering effects.

It has not proven possible to calculate the upward flux of momentum in the horizontal directions, since the vertical perturbations of velocities are not available. However, the covariance of the east-west and north-south perturbation velocities, $\langle \Delta u \Delta v \rangle$, can be calculated to confirm the coherence of phase of any detected gravity waves (e.g., Figs. 1 and 2). An average of the Δu, Δv products over a vertical wavelength (81–105 km), and for 1 hr (approximately 12 profiles), has confirmed the consistency of sign of the covariance. On 15 March, 0900–0955 CST, 8 of the 12 profiles produced a positive covariance, with an overall average of $+400$ m^2 sec^{-2}. For the 1300–1375 CST data, 11 of the 12 profiles evidenced a negative sign, giving an average for the hour of -2000 m^2 sec^{-2}. Several of the other intensive sequences in which phase progressions could be seen also produced large non-zero values of covariance.

A summary of the results of irregular wind analysis for 1972-73 is shown in Table 1. The number of intensive sequences fully processed per month and the characteristics of the waves identified therein, e.g., directions of phase progression, estimates of period (τ), vertical wavelength (λ_z), and amplitude at two selected heights, are shown. With regard to phase progression, monochromatic atmospheric gravity wave observations are not to be expected at these heights; and the fact that many irregular wind profiles do not demonstrate regular phase progression is not inconsistent with the assumption of wave motion as a cause of the irregular components. Also of importance are the percentages of intensive sequences which were suitable for complete processing. Even under automatic operation, the percentage of soundings adequate for processing is extremely high, and makes the method observationally efficient and economical.

The characteristics deduced from the various plots and shown in Table 1, plus the figures which show amplitude increases with height, are appropriate to internal atmospheric gravity waves at "meteor wind heights" (Hines, 1960; Midgley and Liemohn, 1966). Waves with 12 $\lambda_z < 30$ km and $30 < \tau < 60$ min may be resolved with the present system and data, and although all values within these ranges have been identified, the dominant characteristics are given in Table 1. These could, however, be partially a function of observational ease or bias.

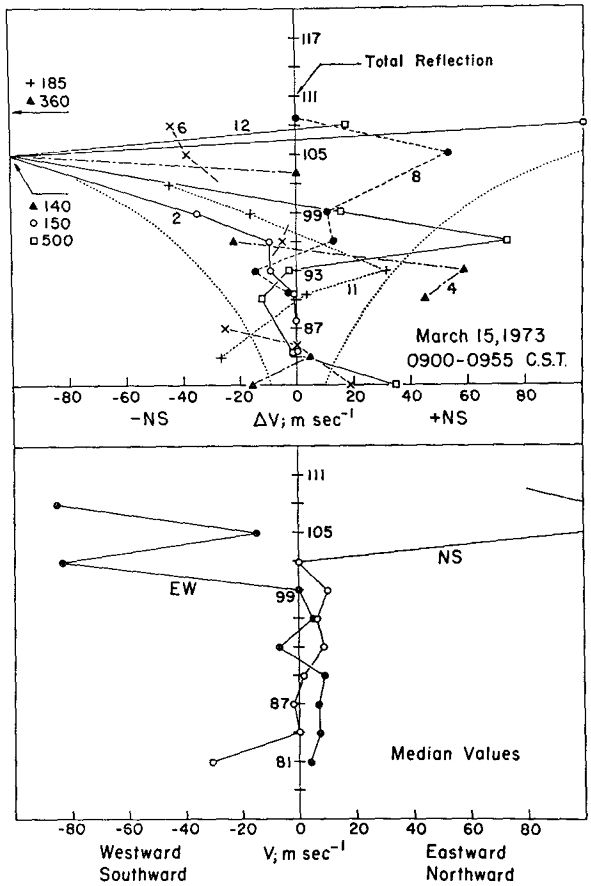

FIG. 2. As in Fig. 1 except for 0900–0955 CST.

5. Seasonal variations in gravity wave parameters

a. *Amplitudes*

The month-by-month variations in the amplitudes of irregular winds can be studied by assembling all of the data from the intensive sequences, and calculating the rms values for the zonal and meridional

TABLE 1. Irregular wind/gravity wave analysis: 1972–73.

	Number of 1-hr runs	Phase progression (%) [horizontal and vertical]	[horizontal]	[irregular]	Periods (min)	Wavelength (km)	Maximum amplitude (m sec^{-1}) ~85 km	~105 km	Intensive sequences processed* (%) Noon	Other
November	3	0	100	0	~60	~20	15	70	100*	—
December	8	0	63	37	~60	~20	35	65	75*	83*
January	8	25	63	12	60	20	25	70	100*	75*
February	4	50	50	0	30–50	20	35	95	50*	80*
March	11	27	55	18	35–50	15–20	25	100	75	31
April	13	23	46	30	50	25	25	90	75	44
May	20	5	65	30	55	~20	<25	50	90	55
June	16	0	31	69	>60	~20	25	70	100*	62*

* Data with an asterisk were obtained by manual operation of the system.

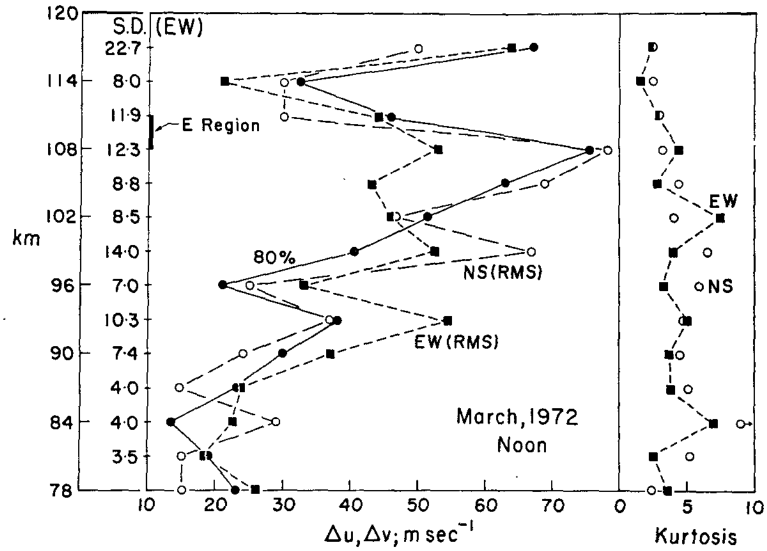

FIG. 3. Irregular wind amplitudes. The statistical terms are described in the text.

components. These showed that diurnal effects were significant, so noon data only were selected. The data for noon periods during March are shown in Fig. 3; a line including the smallest 80% of the values for both components is also plotted. For March (and the other months) there are relatively small differences over this height range between the north-south and east-west amplitudes. In later plots the 80% line is used exclusively, since it reduces the effect of occasional high velocities, is otherwise closely similar to rms values, and therefore provides a useful smoothing of the rms values.

The rms (and 80% line) values and standard deviations of the irregular winds, and also the trend of the kurtosis (the fourth moment of the distribution divided by the variance squared), are in good agreement with those shown by Justus (1970) and Justus and Woodrum (1973). The large values of kurtosis indicate a distribution with a high central peak and broad skirts; the decrease with height may represent the loss of gravity wave modes having small vertical wavelengths and amplitudes below 100 km. The heights shown for winds near the E region ($\gtrsim$102 km) will be in error by several kilometers ($\sim$5 km) due to group retardation effects (Manson *et al.*, 1973). It was considered undesirable to omit these data, but only trends in the winds at these heights should be considered. It should be noted that statistically reliable winds were obtained up to 9 km above the E region, indicating a significant roughness in the height of the critical electron density.

Comparisons of noon data for groupings of months are shown in Fig. 4. An assemblage of all the data provided evidence for a strong diurnal variation, but otherwise an identical month-by-month variation. However, to ensure that the group retardation effects above $\sim$102 km were consistent for each month, the noon data have been presented in preference. Also shown is the perturbation velocity appropriate to a constant energy-density wave. The measured energy varies with height as

$$\rho_0\langle\Delta u^2+\Delta v^2\rangle \propto \exp(-z/z_0),$$

where ρ_0 is the ambient density and z_0 the "scale height." Calculations show that in winter z_0 is $\sim$8 km and in summer $\sim$6 km. These are similar to a mean value of 10 given by Kochanski (1964).

The seasonal variation of amplitudes can be summarized as follows. In general, during the winter months (November–February) the perturbations have their largest values, especially above 108 km in January and February. The variation with height is closest to the constant energy density lines during these months (z_0=7.6). During the equinoxial months of March and April, the height of the maximum perturbations decreases and moves from 108 km in March to 102 km in April. This trend is also apparent in the assemblage of all of the data, and is believed to be significant. Below 102 km, the equinoxial perturbations are the least for the year. Finally during the summer months of May and June, amplitudes below 96 km increase from equinoxial values (while remaining less than winter values) but increase with height at a rate significantly less than in winter (z_0=6.3). Above 108 km, the May values become quite large but fall again in June. These variations will be discussed later in conjunction with the zonal wind time cross sections.

b. Vertical shears

These were obtained from the individual wind profiles by a method originally used by Rosenberg and Zimmerman (1972), and previously applied to radiowave data by Manson *et al.* Estimates of the shears, amplitudes and "wavelengths" were obtained from individual profiles, and then assembled according to height range for groups of profiles. The resulting shears are shown in Fig. 5. Several of the months have been combined to illustrate the winter, equinoxial and summer variations, since profiles with at least five wind determinations were required for the analysis. The diurnal variation in shear was not as significant as for the amplitude, so these data refer to the complete sample. Finally, the points shown refer to the medians of the values occurring in each height-time assemblage, and also the medians of the maxima appropriate to each individual profile. Summer shears are significantly less than those during winter or the equinoxes. These values compare well with the mean vertical shears, based on sodium cloud data presented by Kochanski (1964).

6. Diurnal variation of gravity wave parameters

The irregular wind amplitudes, shears and wavelengths appropriate to individual profiles within each of the intensive sequences, were assembled to illustrate

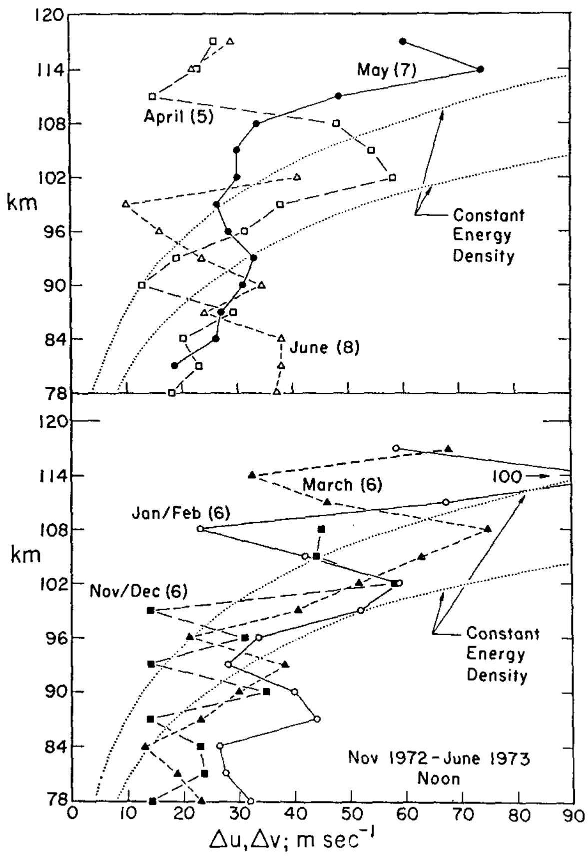

FIG. 4. Irregular wind amplitudes. The number following the month refers to the number of noon soundings per month. The amplitudes are closely similar to rms values.

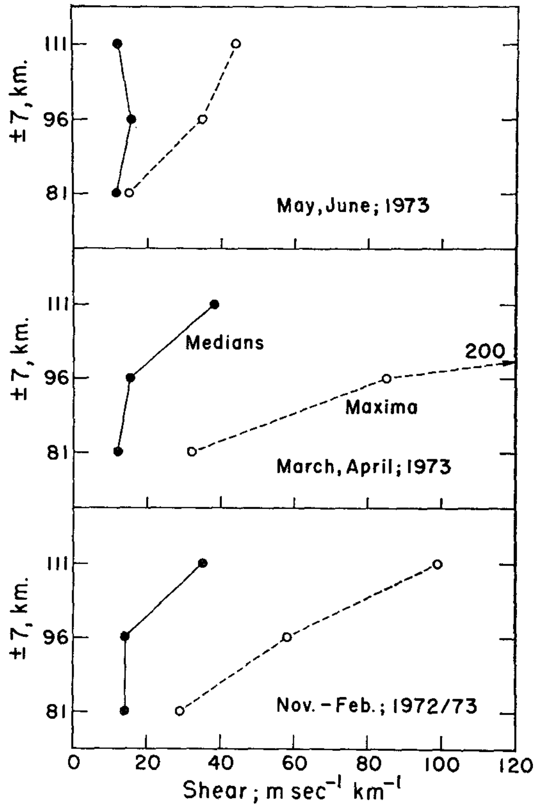

FIG. 5. Vertical shear associated with the irregular wind components. Data at each height are appropriate to a 14-km height interval.

the diurnal variation. The data for April, shown in Fig. 6, are typical of the variations during much of the year, and the differences from season to season will now be summarized for each height range in turn.

1) 104–111 km: During summer and winter the amplitudes, and to a lesser extent the shears, also show noon minima; in winter the amplitude and shear values are larger while in summer the shear values are smaller.

2) 89–103 km: During summer and winter the amplitudes also pass through noon minima, although they are much less regular than in the 104–111 km region; the shear is also irregular, although some noon minima are evident. The winter amplitudes are larger, while the summer values are similar to those of April.

3) 74–88 km: The summer and winter curves do *not* show any diurnal trend; summer and winter amplitudes and shears are close to the April noon values.

In general, then, the amplitudes and shears associated with the irregular winds evidence a diurnal variation which is increasingly evident above 90 km; superimposed upon this are the seasonal variations in amplitude and shear which were discussed in the previous section.

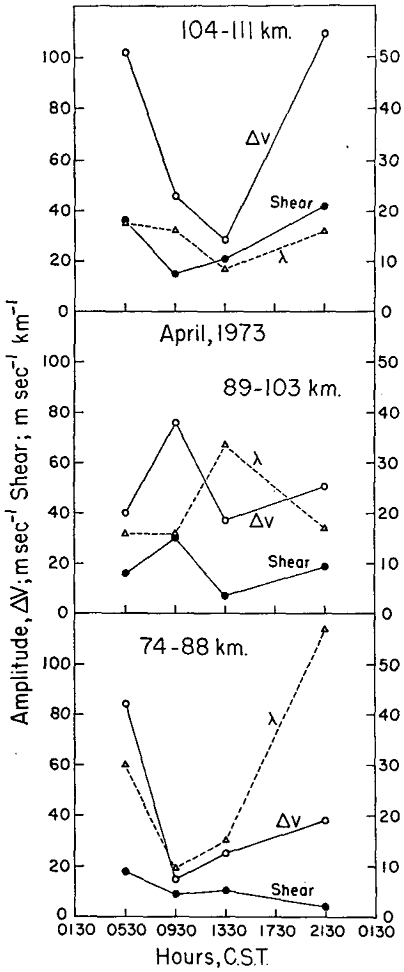

FIG. 6. Amplitudes (ΔV), shears, and vertical wavelengths (λ_z) associated with irregular wind components.

7. Gravity wave parameters in relation to prevailing winds

a. Data

There has been much interest recently in the effect of a mean horizontal flow on the propagation of internal gravity waves (Eliassen and Palm, 1961; Booker and Bretherton, 1967; Hines and Reddy, 1967). Also of interest is the means by which waves transport momentum and produce changes in the mean state of the atmosphere (e.g., Jones and Houghton, 1971, 1972; Hines, 1972).

The median winds available from the one hour intensive sequences have been used to form the time cross section of zonal winds shown in Fig. 7. The weekly mean profile subsequent to January is a combination of two adjacent midweek profiles. Systematic trends are evident. The meridional time cross section, which is not shown here, also shows systematic seasonal trends, but the magnitudes are in general much smaller. The winds below 70 km have been obtained from ROCOB data for 54N, 110W (Primrose Lake, Alberta), and also refer to one or two firings per week in this period. The consistency between these two sets of data is extremely good. It should again be noted that above 102 km group retardation effects contribute to a decrease in the height of the calculated wind, and values should be corrected by ~5 km: the upper virtual height of 117 km is probably closer to 110 km actual height. The amplitude and shear associated with the irregular wind components is also shown for the individual weeks. The seasonal and altitude variations which have been discussed in detail above are also evident from this presentation.

It is of interest to compare the seasonal variation of irregular wind amplitudes available from Fig. 4, with the noon zonal winds of Fig. 7. There is some indication of a relationship between the height of reversal for the eastward (positive) and westward (negative) winds, and the height of the maxima for the irregular winds in Fig. 4. From January–February through March and April both of these variables reduce systematically in height, the irregular wind maxima being several kilometers higher than the reversal height for the zonal flows. (However, it should be noted that the amplitude of the irregular March winds is increasing from 114 to 117 km, a trend which if it were to continue, would break this systematic height reduction.) Again, during the month of May, the westward flow is established to over 100 km, and the height of the maximum for the irregular wind amplitudes for that month has also increased to 108 km. The height and variation of the reversal from northward to southward flow in the meridional time cross section, is comparable to that for the zonal winds for the months March–May.

A preliminary study of a selection of data from 1973–74 also provides evidence for interactions between gravity waves and the mean wind. However, it appears that although there may be correspondence between significant *features* of the irregular wind profile and the mean wind directions, the amplitude of the irregular wind may increase again at greater heights. A change in the spectrum with height will also probably occur. This is an indication of the complexity of the dynamical processes which are involved.

b. Discussion

The theory of interactions between the mean wind and gravity waves is quite well developed. Jones and Houghton (1971, 1972) have shown, by means of numerical modelling, that for a steady-state periodic wave, a discontinuity in the upward flux of horizontal momentum (Reynolds stress) occurs at a critical level (where the mean flow velocity equals the phase velocity of the wave). Also, if a more realistic wave packet is considered, and dissipation effects are involved, a residual momentum is left in the mean flow.

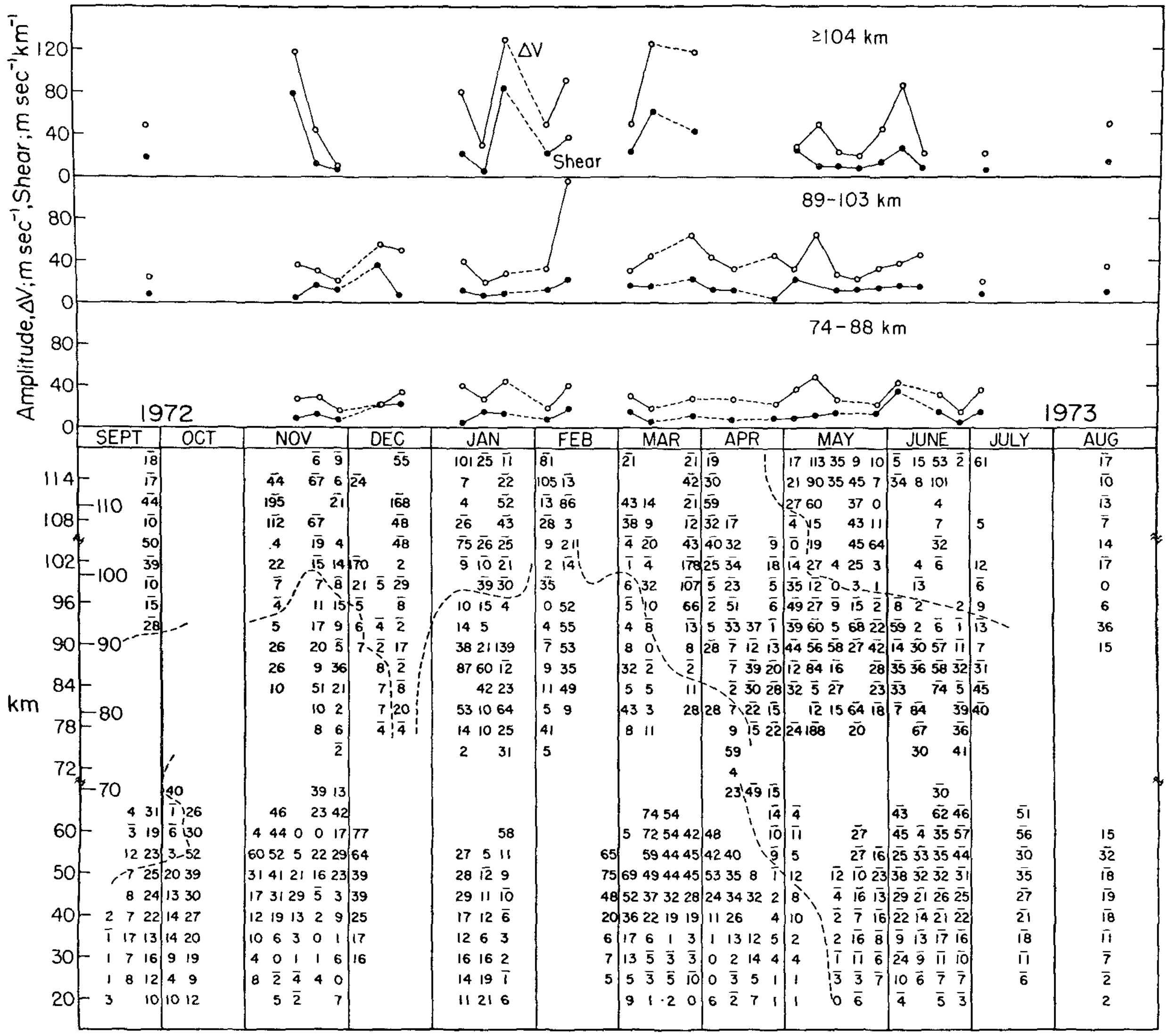

FIG. 7. Time cross section of median zonal winds at noon (the bar indicates a negative or westward wind), showing the height of reversal between eastward (+) and westward winds (−). The amplitudes (ΔV) and shear associated with the irregular wind components are plotted above.

This could modify or create a critical layer interaction.

It also seems likely that for the gravity waves identified here (Section 4), interaction with winds and reflection due to temperature gradients below 100 km will be the dominant loss mechanisms. Molecular viscosity and thermal conductivity will cause significant dissipation above 100 km (Hines, 1960). In view of these factors, it is conceivable that the rapid decrease in height of the east-west transition in the zonal flow is due to the absorption of momentum from a gravity wave flux, in a similar manner to that suggested by Lindzen and Holton (1968) and Lindzen (1971) with regard to the equatorial quasi-biennial oscillation. An alternate and associated possibility is that the maxima (or significant features) in the gravity wave amplitudes are associated with critical levels near the east-west transition in the zonal flow (Figs. 4 and 7).

Local conditions of convection or shear instability, which lead to the formation of turbulence, may also be existent when gravity waves reach a certain amplitude (Hines, 1963; Hodges, 1967). It is possible that dissipation of gravity waves due to this type of process may have been occurring, since the wave characteristics (Section 4) are similar to those used by Hodges for his calculations of instability. This would certainly account for the dissipation of the waves with altitude ($z_0 = 6.3-7.6$) and lead to heating of the atmosphere via kinematic viscosity. Dissipation of wave packets would also lead to a residual momentum being left in the mean flow (Jones and Houghton,

1972) at heights other than the critical level. Observations involving several consecutive hours of intensive runs, allowing comparisons between the development of the mean flow and the gravity wave flux, will be required to answer and verify some of these suppositions.

8. Tropospheric sources for gravity waves

An attempt was also made to locate the source of the gravity wave fluxes detected during 1972–73. Using the asymptotic simplifications for gravity wave characteristics developed by Hines (1960), the horizontal wavelength ($\lambda_x \approx 200$ km) and phase velocity ($V_p \approx 60$ m sec^{-1}) may be calculated for the dominant modes discussed in previous sections. The angle of propagation is approximately 6° above the horizontal. Using a ray-tracing technique similar to that discussed by Hines (1968), the source of gravity waves could be located as lying in the eastern foothills of the Canadian Rockies, toward the center of Alberta, at the time of noon ionospheric observations in Saskatchewan. The surface weather maps and 300-mb pressure charts were studied for evidence of unusual frontal or jet-stream activity, respectively. For November–March there were indications of a relationship between the presence of highly developed surface high and low pressure systems in Alberta and their associated cold and warm frontal systems, and the instances of maxima in the irregular wind amplitudes (Fig. 7). These results are consistent with those discussed by Hines, but suffer from a similar difficulty in identifying the angle of arrival of the individual gravity waves. Experimental systems involving angle-of-arrival systems are likely to improve this uncertainty.

9. Discussion and conclusion

The identification of gravity waves in the upper atmosphere (80–105 km), which was discussed elsewhere (Manson *et al.*, 1973), is considered as confirmed by analysis of the winds data for 1972–73. These data have involved some of the first closely spaced soundings of this region of the upper atmosphere. It is now clear that gravity wave activity is an extremely frequent and important feature of the dynamics of the mesosphere and lower thermosphere. The altitude variations of amplitudes and shears associated with the gravity waves reported here evidence good agreement with results obtained from individual rocket wind profiles (Kochanski, 1964; Justus and Woodrum, 1973). Also, the inferred vertical wavelengths, periods and amplitudes are consistent with those for suggested dominant modes at these heights (Hines, 1960; Midgley and Liemohn, 1966).

Significant diurnal and seasonal variations in the gravity wave amplitudes and shears have been demonstrated. Physical explanations for these would be conjectural at this stage. However, observational confirmation for the maximum winter amplitudes could lie with the evidence for winter variability in neutral atmosphere parameters (Theon *et al.*, 1967) and ionospheric (60–100 km) parameters (Gregory and Manson, 1969). The diurnal variation is unexpected. A possible explanation involves a diurnal variation in the group retardation correction, which could introduce an apparent diurnal amplitude variation if a strong positive gradient of amplitudes exists near 110 km. In fact, the opposite is likely (Kochanski, 1964). However, there is some other observational evidence for a diurnal variation, in meteor winds data. Barnes and Pazniokas (1972) show diurnal curves for 2-hr means and standard deviations for several months. The standard deviations, which will be largely due to gravity waves, tend to have their largest values during night hours, even though the number of observations also maximize then.

Finally, interactions between gravity waves and the zonal flow have been suggested, and also possible identifications made with tropospheric sources of these waves. There is considerable theoretical justification for such relationships. Improvements in the radiowave sounding system to allow direction finding and horizontal scale measurements are planned, to allow elaboration upon these atmospheric processes.

Acknowledgments. The authors wish to acknowledge the support of the National Research Council of Canada and the Atmospheric Environment Service. The use of University of Saskatchewan facilities is also gratefully acknowledged.

REFERENCES

Barnes, Jr., A. A., and J. J. Pazniokas, 1972: Results from the AFCRL radar meteor trail set. AFCRL Environmental Research Paper No. 392, 81 pp.

Booker, J. R., and F. P. Bretheron, 1967: The critical layer for internal gravity waves in a shear flow. *J. Fluid Mech.*, **27**, 513–539.

Chapman, S., and R. S. Lindzen, 1970: *Atmospheric Tides*. New York, Gordon and Breach, 200 pp.

Elford, W. G., 1959: A study of winds between 80 and 100 km in medium latitudes. *Planet. Space Sci.*, **1**, 94–101.

Eliassen, A., and E. Palm, 1961: On the transfer of energy in stationary mountain waves. *Geofys. Publ.*, **22**, No. 3, 1–23.

Fraser, G. J., 1968: Seasonal variations of Southern Hemisphere mid-latitude winds at altitudes of 70–100 km. *J. Atmos. Terr. Phys.*, **30**, 707–720.

Gregory, J. B., and A. H. Manson, 1969: Seasonal variations of electron densities below 100 km at mid-latitudes—II. Electron densities and atmospheric circulation. *J. Atmos. Terr. Phys.*, **31**, 703–729.

——, and D. T. Rees, 1971: Wind profiles to 100 km near 53N during 1969. *J. Atmos. Sci.*, **28**, 1079–1082.

——, and D. G. Stephenson, 1972: High altitude winds from radio reflections. *Can. Res. Develop.*, March/April.

——, A. H. Manson and D. G. Stephenson, 1973: High altitude winds and tides at Saskatoon, Canada. Rept. No. 3, Atmos. Dyn. Group, ISAS, University of Saskatchewan, 43 pp.

Groves, G. V., 1969: Wind models from 60 to 130 km altitude for different months and latitudes. *J. Brit. Interplanet. Soc.*, **22**, 285–307.

Hines, C. O., 1960: Internal atmospheric gravity waves at ionospheric heights. *Can. J. Phys.*, **38**, 1441–1481.
——, 1963: The upper atmosphere in motion. *Quart. J. Roy. Meteor. Soc.*, **89**, 1042–1083.
——, 1968: A possible source of waves in noctilucent clouds. *J. Atmos. Sci.*, **25**, 937–942.
——, 1972: Momentum deposition by atmospheric waves, and its effect on thermospheric circulation. *Space Research XII*, S. A. Bowhill *et al.* Eds., Berlin, Akademie-Verlag, 1157–1161.
——, and C. A. Reddy, 1967: On the propagation of atmospheric gravity waves through regions of wind shear. *J. Geophys. Res.*, **72**, 1015–1034.
Hodges, Jr., R. R., 1967: Generation of turbulence in the upper atmosphere by internal gravity waves. *J. Geophys. Res.*, **72**, 3455–3458.
Jones, W. L., and D. D. Houghton, 1971: The coupling of momentum between internal gravity waves and mean flow: A numerical study. *J. Atmos. Sci.*, **28**, 604–608.
——, and ——, 1972: The self-destructing internal gravity wave. *J. Atmos. Sci.*, **29**, 844–849.
Justus, C. G., 1970: Distribution and structure of irregular winds near 100 kilometers. *J. Geophys. Res.*, **75**, 2171–2178.
——, and A. Woodrum, 1973: Short and long period atmospheric variations between 25 and 200 km. NASA Contractor Rept. CR-2203, 86 pp.
Kochanski, A., 1964: Atmospheric motions from sodium cloud drifts. *J. Geophys. Res.*, **69**, 3651–3662.
Lindzen, R. S., 1971: Equatorial planetary waves in shear: Part I. *J. Atmos. Sci.*, **28**, 609–622.
——, and J. R. Holton, 1968: A theory of the quasibiennial oscillation. *J. Atmos. Sci.*, **25**, 1095–1107.
Manson, A. H., J. B. Gregory and D. G. Stephenson, 1973: Winds and wave motions (70–100 km) as measured by a partial reflection radiowave system. *J. Atmos. Terr. Phys.*, **35**, 2055–2067, 1973.
Midgley, J. E., and H. B. Liemohn, 1966: Gravity waves in a realistic atmosphere. *J. Geophys. Res.*, **71**, 3729–3748.
Rosenberg, N. W., and S. P. Zimmerman, 1972: Ionospheric winds and viscous dissipation. *Radio Sci.*, **7**, 377–380.
Stubbs, T. J., 1973: The measurement of winds in the D-region of the ionosphere by the use of partially reflected radio waves. *J. Atmos. Terr. Phys.*, **35**, 909–919.
Theon, J. S., W. Nordberg, L. B. Katchen and J. J. Horvath, 1967: Some observations of the thermal behavior of the mesosphere. *J. Atmos. Sci.*, **24**, 428–438.